Microwave Zeeman Effect of Free Hydroxyl Radicals: $^2\Pi_{\frac{1}{2}}$ Levels*

H. E. RADFORD
National Bureau of Standards, Washington, D. C.
(Received June 21, 1961)

Two new paramagnetic resonance spectra of the free $O^{16}H$ radical have been observed at 3 cm wavelength in the products of an electric discharge in water vapor. The spectra arise from Λ-type doubling transitions in the $^2\Pi_{\frac{1}{2}}$, $J=\frac{3}{2}$ and $^2\Pi_{\frac{1}{2}}$, $J=\frac{5}{2}$ levels. Molecular magnetic moments and hyperfine structure constants measured from the spectra lead to refinements in the theory developed earlier to account for similar measurements on $^2\Pi_{\frac{1}{2}}$ levels. A consistent analysis of the combined $^2\Pi_{\frac{1}{2}}$ and $^2\Pi_{\frac{3}{2}}$ data is then possible, and yields the following major results. From the measured magnetic moments we find $g_s(\mathrm{OH})=g_s(\text{free electron})\pm0.0002$, $\lambda=-7.504\pm0.003$, where $g_s(\mathrm{OH})$ is the spin g factor of a molecular electron and λ is the ratio of the spin-orbit coupling constant to the rotational constant of the ground state. This value of λ disagrees with an earlier microwave measurement. Values of matrix elements connecting the ground and first excited electronic states are also derived from the measured magnetic moments. Analysis of the hyperfine structure yields the molecular constants (in units of 10^{24} cm^{-3}): $\langle 1/r^3\rangle_\pi=(1.089\pm0.008)$, $\Psi^2(0)=(0.113\pm0.001)$, $\langle(3\cos^2\chi-1)/r^3\rangle=(1.125\pm0.008)$, and $\langle\sin^2\chi/r^3\rangle=(0.477\pm0.003)$, which describe the distribution of unpaired electrons about the hydrogen nucleus. The hyperfine structure is perturbed rather strongly by configuration interaction.

I. INTRODUCTION

THE magnetic moments of free paramagnetic molecules come mainly from the spin and orbital magnetism of their unpaired electrons. Knowing the coupling scheme of the electronic angular momenta, one can usually predict the magnetic moment of a given molecular level within a few parts in 10^3. Theory is far behind experiment in this respect, for the magnetic moments of some paramagnetic molecules can be measured by microwave methods to a precision exceeding 1 part in 10^5. The obstacle to better theoretical precision, and thus to a better understanding of the experimental results, is the generally poor knowledge of molecular wave functions. The kinematic effect of molecular rotation on the electronic wave function is particularly hard to calculate, and instead must be derived, in a more or less uncertain fashion, from measurements of phenomena such as the rotational distortion of spin multiplets or the Λ-type doubling of individual rotational levels.

In the hydroxyl radicals, rotational distortion of the ground $^2\Pi$ electronic state is rather pronounced, and the Λ-type doublet splittings fall in the microwave range, where they can be measured with the full precision of the microwave absorption method. Other workers[1,2] have devoted considerable effort to measuring and interpreting these splittings, and the results include most of the information on wave functions that is necessary for a precise calculation of molecular magnetic moments. The large Λ-type doublet splittings also make the most common hydroxyl radical, $O^{16}H$, especially amenable to study by the convenient technique of paramagnetic resonance absorption at 3 cm wavelength. Although the Λ-type doublet and Zeeman effect splittings vary widely among the different $O^{16}H$ molecular levels, the sum (or difference) of the two splittings at magnetic field strengths of a few thousand gauss remains tolerably near 9 kMc/sec for several of the lowest levels. Exact paramagnetic resonance can be established in five different levels through a moderate variation of the magnetic field strength. By thus observing the Zeeman effect of the Λ-type doubling absorption, one can measure the magnetic moments of all five levels under nearly identical conditions.

In an earlier paper[3] (referred to as R1 hereafter) we reported paramagnetic resonance measurements on three of these levels—the three lowest $^2\Pi_{\frac{3}{2}}$ levels [the terminology of Hund's case (a) coupling is convenient and will be used here, although the actual coupling deviates considerably from this ideal case]. The major purpose of the experiment was to measure the spin magnetic moment of an electron in the axially symmetric environment provided by a diatomic molecule. An environmental effect on the spin moment, if present at all, should show up most clearly in a molecule such as OH, where a first-order spin-orbit interaction couples the spin vector firmly to the molecular axis. The measured magnetic moments of the three levels did, in fact, differ considerably from those calculated with the free-electron value of the spin moment and wave functions deduced from the zero-field microwave absorption experiments. If the wave functions were assumed to be correct, the spin moment derived from the comparison of theory with experiment turned out to be precisely one Bohr magneton within an uncertainty of ±1 part in 10^4, rather than $1.0016\,\mu_0$, the well-known anomalous moment of the free electron. This is certainly an interesting result, but it should not be fully believed before subjecting the wave functions to adequate independent tests for accuracy. Lacking such tests, we could reach no firm conclusion in R1 regarding the source of the discrepancy between theory and experiment.

* This work was supported in part by the Office of Naval Research.
[1] G. C. Dousmanis, T. M. Sanders, Jr., and C. H. Townes, Phys. Rev. **100**, 1735 (1955).
[2] G. Ehrenstein, C. H. Townes, and M. J. Stevenson, Phys. Rev. Letters **3**, 40 (1959).
[3] H. E. Radford, Phys. Rev. **122**, 114 (1961). In the present paper this earlier work is referred to as R1.

The two remaining OH levels accessible to our apparatus are nominal $^2\Pi_{\frac{1}{2}}$ levels; their absorption spectra, much weaker than the $^2\Pi_{\frac{3}{2}}$ spectra, could not be observed in the earlier experiment. Through improvements in the technique of producing OH radicals, we have now succeeded in observing and analyzing these spectra. The results complement the earlier work on $^2\Pi_{\frac{3}{2}}$ levels in a much deeper sense than that of just providing data on two more rotational levels. The reason is the following: In a pure $^2\Pi_{\frac{3}{2}}$ level the electron orbital and spin magnetism reinforce each other and give the level a large magnetic moment—for a total molecular angular momentum (excepting nuclear spin) specified by the quantum number J, the moment is $-3\,\mu_0[J(J+1)]^{-\frac{1}{2}}$. In a pure $^2\Pi_{\frac{1}{2}}$ level, however, the spin and orbital magnetism oppose each other, and the net magnetic moment is essentially zero. Now, in the hydroxyl radicals the $^2\Pi_{\frac{3}{2}}$ level and the $^2\Pi_{\frac{1}{2}}$ level labeled by the same value of J are by no means pure, but, because of rotational distortion, each contains an admixture of the other, i.e., the coupling is intermediate between Hund's cases (a) and (b). The magnetic properties are also mixed, the impure $^2\Pi_{\frac{1}{2}}$ level borrowing an electronic magnetic moment from the impure $^2\Pi_{\frac{3}{2}}$ level. This is where the need for adequate wave functions arises, for the magnetic moments of the impure levels cannot be calculated without knowledge of the level admixture, which is provided by the wave functions. However, and this is the point of the present experiment, to calculate the *sum* of the magnetic moments of the two admixed levels no such knowledge is required; this sum retains the case (a) value $-3\,\mu_0[J(J+1)]^{-\frac{1}{2}}$ regardless of rotational distortion. A more careful analysis adds several small corrections to this theoretical sum, but the major conclusion remains plain: The measured magnetic moment sums may be interpreted without recourse to wave functions. This provides the key to an understanding of the discrepancies between theory and experiment noted in R1.

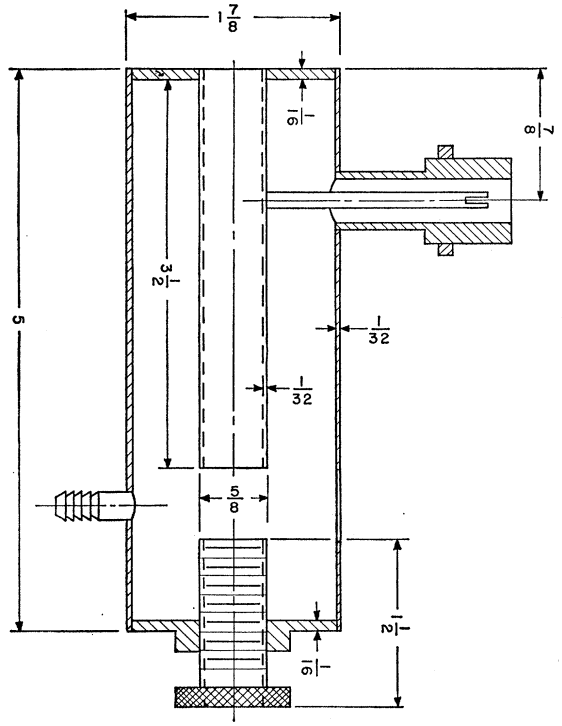

FIG. 1. Re-entrant cylindrical resonator used to produce hydroxyl radicals in the present experiment. An electric discharge is excited at the re-entrant gap in a coaxial glass tube carrying water vapor. The power source is a 2450 Mc/sec diathermy generator, connected to the rf jack on the right. The resonator is tuned by varying the length of the re-entrant gap with the threaded insert. The material is brass; joints are hard-soldered. Forced air cooling is necessary.

The paramagnetic resonance spectra of hydroxyl radicals also exhibit hyperfine structure (hfs), due to the interaction of the proton or deuteron (other isotopic substitutions were not made) magnetic moment with the valence electrons of the molecule. In R1 the hfs splittings were analyzed in terms of four coupling constants, called a, b, c, and d, which depend on the spatial distribution of valence electrons about the magnetic nucleus. The $^2\Pi_{\frac{3}{2}}$ spectra alone were inadequate to determine the numerical values of all four constants, but with the auxiliary theoretical relation $c=3(a-d)$ a consistent set of values could be derived from the spectra. The use of this auxiliary relation amounts to the assumption that the same electrons are responsible for both the orbital and spin contributions to the hfs. The hfs of the $^2\Pi_{\frac{1}{2}}$ spectra now show that this assumption is not at all true, and, accordingly, that the hfs constants derived in R1 are wrong. Correct values of the four hfs constants, derived from the combined $^2\Pi_{\frac{1}{2}}$ and $^2\Pi_{\frac{3}{2}}$ data, show that the failure of the relation $c=3(a-d)$ in the hydroxyl radicals is caused by rather strong effects of configuration interaction.

II. EXPERIMENT

1. Apparatus

The $^2\Pi_{\frac{1}{2}}$ paramagnetic resonance spectra were observed in the products of a microwave electric discharge in water vapor, which were pumped continuously through the cavity of a Varian V-4500 EPR spectrometer. The only essential change in the experimental arrangement over that described in R1 was in the type of discharge resonator employed: The rectangular waveguide resonator was replaced by a re-entrant cylindrical resonator which delivered, for reasons unknown, about three times as many hydroxyl radicals to the spectrometer cavity at the same total pressure. Construction details of the new resonator, which was designed by H. P. Broida, are given in Fig. 1. Qualitative tests on other gases (nitrogen, oxygen and hydrogen) suggest the general superiority of this resonator design over the waveguide type for the production of any gaseous radical. The range of pressures over which a discharge can be maintained is extremely broad, extending from a

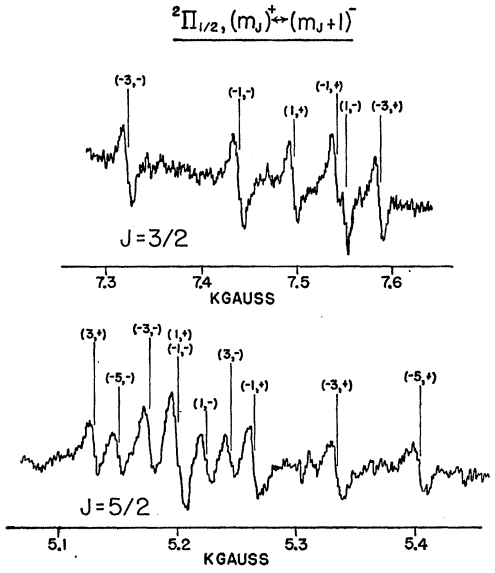

FIG. 2. Paramagnetic resonance spectra of $O^{16}H$, $^2\Pi_{\frac{1}{2}}$ levels. Microwave frequency: 9200 Mc/sec.

few microns to 200 mm Hg in the case of air or nitrogen, with a power input of 125 watts at 2450 Mc/sec. The re-entrant design keeps the resonator small in size and also concentrates the electric energy in a small axial region, just where it is needed to excite the discharge; presumably this is the reason for the broad operating range of pressure.

2. The $^2\Pi_{\frac{1}{2}}$ Spectra

With the higher radical concentration provided by the re-entrant resonator, the two $^2\Pi_{\frac{1}{2}}$ absorption spectra were strong enough to be located in a reasonably short search time. Signal amplitudes were found to depend critically on the water vapor pressure and the microwave power level in the discharge; an optimum signal-to-noise ratio of about 20 was achieved for individual lines of the $J=\frac{3}{2}$ spectrum, the stronger of the two, at a vapor pressure of $\frac{1}{2}$ mm Hg and a discharge power input of 10 watts. Typical derivative recordings of the spectra are shown in Fig. 2. These recordings were made at vapor pressures of roughly $\frac{1}{4}$ mm Hg, at some sacrifice of signal-to-noise ratio, so as to reduce pressure broadening. Although some of the lines are still incompletely resolved at this pressure, the resolution is adequate for our purposes. The linewidths, measured in gauss, are much larger than those of the $^2\Pi_{\frac{1}{2}}$ spectra; this is partly because of the higher pressures that were required here, but more especially because the widths of paramagnetic resonance lines are inversely proportional to the effective magnetic moment involved, and the magnetic moments of the $^2\Pi_{\frac{1}{2}}$ levels are rather small. The equivalent frequency widths of the lines in Fig. 2, measured between the derivative maxima, are about 2 Mc/sec. The positions of the lines in these spectra were measured several times, under different experimental conditions, using the proton resonance and frequency-counting techniques described in R1.

The $^2\Pi_{\frac{1}{2}}$ levels that give rise to these spectra are marked with double asterisks in Fig. 3, which shows the disposition of the lowest levels of OH and OD; single asterisks mark the $^2\Pi_{\frac{3}{2}}$ levels with which R1 was concerned. (The single $J=\frac{1}{2}$ level of each molecule is a pure $^2\Pi_{\frac{1}{2}}$ level, and is not paramagnetic.) The Λ-type doubling of each level is exaggerated for clarity, but hyperfine splittings are omitted. In an external magnetic field each hyperfine component splits further into several magnetic sublevels. A magnified picture of this Zeeman splitting for the ground level of OH is shown in R1; in general one ends up with two groups of $(2I+1)(2J+1)$ sublevels separated by the Λ-type doubling interval. The spectra of Fig. 2 correspond to electric dipole transitions between these two groups of sublevels, governed by the usual paramagnetic resonance selection rules $\Delta m_J=\pm 1$, $\Delta m_I=0$; the somewhat cryptic title $(m_J)^+ \leftrightarrow (m_J+1)^-$ on Fig. 2 refers, in the notation of R1, to the fact that the Λ-type doubling and Zeeman effects add in this case to make up the transition energy of 9 kMc/sec. Each spectrum has a counterpart in which the two effects subtract, but these spectra are out of reach at extremely high field strengths. The individual lines in Fig. 2 have abbreviated labels that give the value of $2m_J$ for the upper sublevel involved in the transition, followed by the value of m_I: A plus sign means $m_I=+\frac{1}{2}$ and a minus sign means $m_I=-\frac{1}{2}$. This assignment of quantum numbers follows directly from the relative magnitudes of the line separations, which are unequal because of hyperfine doubling effects.

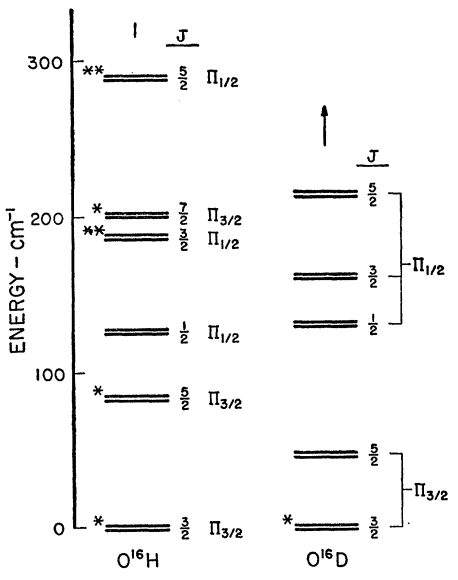

FIG. 3. Lowest fine structure-rotational levels of $O^{16}H$ and $O^{16}D$. The small Λ-type doubling intervals are exaggerated for clarity. Levels marked with single asterisks were investigated earlier. The $^2\Pi_{\frac{1}{2}}$ levels discussed in this paper are marked with double asterisks.

TABLE I. Experimental results for $^2\Pi_{\frac{1}{2}}$ levels. Molecular g factors, coefficients of the quadratic Zeeman effect, and hfs coupling constants derived from the $O^{16}H$ paramagnetic resonance spectra.

	$J=\frac{3}{2}$	$J=\frac{5}{2}$
$(g_J^+ + g_J^-)/2$	-0.13393 ± 0.00002	-0.14113 ± 0.00003
$g_J^- - g_J^+$	0.00099 ± 0.00001	-0.00042 ± 0.00001
K_2	$(6.6 \pm 0.1) \times 10^{-4}$	$(4.1 \pm 0.1) \times 10^{-4}$
$\lvert A_1 \rvert$ (Mc/sec)	20.55 ± 0.06	15.14 ± 0.03
$\lvert A_2 \rvert$ (Mc/sec)	14.56 ± 0.05	9.03 ± 0.03

3. Analysis and Results

The transition energy equation that describes the spectra of Fig. 2 is $h\nu = W^+(m_J, m_I) - W^-(m_J+1, m_I)$ where W^+ and W^-, the energies of the upper and lower sublevels involved in the transition, are given essentially by Eq. (13) of R1. However, because of the relatively small Zeeman effect of the $^2\Pi_{\frac{1}{2}}$ levels it is necessary to modify R1 (13) slightly to account for hyperfine interactions between neighboring Zeeman sublevels. A second-order perturbation calculation suffices, and yields the extra energy term

$$\Delta W^{\pm} = -\tfrac{1}{2} m_I [(J+\tfrac{1}{2})^2 - (m_J + m_I)^2] \times (A_1 \pm A_2)^2 / (g_J - g_I)\mu_0 \mathcal{H},$$

which is to be added to R1 (13). The contribution of this term to the transition energies does not exceed 1.5 Mc/sec, somewhat less than one line width.

A detailed analysis of the spectra, following the method described in R1, yields numerical values of g_J^+ and g_J^-, the molecular g factors of the upper and lower levels of the Λ-type doublet, as well as the two hfs constants A_1 and A_2, and the coefficient of the quadratic Zeeman effect, K_2. Higher order Zeeman effects are negligible. Since the transition energies involve jointly the Zeeman effect and the Λ-type doublet splittings, accurate values of the latter are required in deriving the g factors from the spectra. These splittings, designated by ν_Λ when expressed in frequency units, have been measured by the zero-field absorption method,[1] and are: $\nu_\Lambda(^2\Pi_{\frac{1}{2}}, J=\frac{3}{2}) = 7797.59 \pm 0.15$ Mc/sec and $\nu_\Lambda(^2\Pi_{\frac{1}{2}}, J=\frac{5}{2}) = 8166.08 \pm 0.15$ Mc/sec. Less precise values of ν_Λ can also be found by observing the shift in the location of the paramagnetic resonance spectra as the 9-kMc/sec klystron oscillator is tuned over its frequency band; these were found to agree, within an experimental uncertainty of ± 2 Mc/sec, with the zero-field measurements.

The experimental results are listed in Table I. Instead of the individual g factors, the mean values $(g_J^+ + g_J^-)/2$ and the differences $(g_J^- - g_J^+)$ are given; these combinations, which can be derived directly from the spectra as easily as can the individual g factors, are convenient for later comparison with theory. The numerical values in Table I are mean results of six independent recordings of each spectrum. The five constants derived from each recording account successfully for the measured position of each line of the six-line $J=\frac{3}{2}$ spectrum and the ten-line $J=\frac{5}{2}$ spectrum. Statistical standard errors are quoted in Table I with the values of $(g_J^- - g_J^+)$, K_2, A_1, and A_2, which depend only on measurements of the line separations. Errors quoted with the mean g factors include the stated uncertainties in the zero-field measurements of ν_Λ, as well as the statistical uncertainty of the present measurements. Systematic errors in absolute magnetic field measurements, important in R1, are negligible here because of the large magnetic field widths of the spectral lines; the magnetic field strength could be measured much more accurately than it could be set to the center of a line.

III. COMPARISON WITH THEORY

1. The g-Factor Sums

On summing the theoretical g-factor expressions (8) and (9) of R1, one finds that all terms involving the spin-uncoupling parameter λ cancel out, leaving

$$\bar{g}_J(^2\Pi_{\frac{3}{2}}) + \bar{g}_J(^2\Pi_{\frac{1}{2}}) = [J(J+1)]^{-1}\{3 + 2[4J(J+1)-1](\Pi|L_y|\Sigma^+) \times (\Pi|BL_y|\Sigma^+)/E + \tfrac{1}{2}g_N[4J(J+1)-5] + \tfrac{1}{2}(g_s-2) - 3\langle T\rangle/mc^2\}, \quad (1)$$

where $\bar{g}_J$ means $(g_J^+ + g_J^-)/2$, the mean g factor of the Λ-type doublet. Since the molecular g factors are defined in terms of the magnetic moments μ_J by the relation $g_J = -[J(J+1)]^{-\frac{1}{2}}\mu_J/\mu_0$, the first term of Eq. (1) is just the approximate sum discussed in Sec. I. The remaining terms are written in the order of descending size, and are corrections for:

(a) **L** uncoupling, i.e., rotational uncoupling of the electronic orbital angular momentum from the molecular axis. This effect, which also produces the Λ-type doubling, may be represented by a small admixture of excited $^2\Sigma$ and $^2\Delta$ molecular states into the ground $^2\Pi$ state; since these different states are also coupled by the Zeeman interaction, energy cross terms of appreciable size can result. Both here and in R1 we consider explicitly only one of these foreign states, the $^2\Sigma^+$ at an excitation energy $E = 32682.5$ cm^{-1}. Other more highly excited $^2\Sigma$ and $^2\Delta$ states may also affect the ground state magnetic moments slightly, but an *a priori* estimate of their contribution is difficult without knowledge of their excitation energies.

(b) Nuclear rotation. The preceding term (a) corrects for the rotational magnetic moment of electrons that participate in the end-over-end rotation of the molecule; a similar correction must be made for the magnetic moment produced by rotation of the charged nuclei about their center of mass. For OH the nuclear rotational magnetic moment is very nearly that of a rotating proton, one nuclear magneton. The corresponding g factor to be inserted in (1) is $g_N = -5.42 \times 10^{-4}$.

TABLE II. Comparison of the theoretical g-factor sums, $\bar{g}_J(^2\Pi_{\frac{3}{2}})+\bar{g}_J(^2\Pi_{\frac{1}{2}})$, with experiment.

	$J=\frac{3}{2}$	$J=\frac{5}{2}$	
$3/[J(J+1)]$	0.80000	0.34286	
(a) **L** uncoupling	0.00192	0.00199	
(b) Nuclear rotation	−0.00073	−0.00094	
(c) Spin-moment anomaly	0.00031	0.00013	
(d) Relativistic	−0.00010	−0.00004	
	0.80140	0.34400	Theory
$\bar{g}_J(^2\Pi_{\frac{3}{2}})_{\text{exp}}$	0.93557[a] ±0.00003	0.48529[a] ±0.00015	
$\bar{g}_J(^2\Pi_{\frac{1}{2}})_{\text{exp}}$	−0.13393 ±0.00002	−0.14113 ±0.00003	
	0.80164 ±0.00004	0.34416 ±0.00015	Experiment

[a] Taken from Table II of R1.

(c) The anomalous spin magnetic moment of the electron. A recent direct measurement[4] of $\frac{1}{2}(g_s-2)$ for the free electron yields the value 0.0011609 ± 0.0000024, in good agreement with theory. An environmental alteration of the electron spin moment in OH would show up as a deviation of $\frac{1}{2}(g_s-2)$ from this value.

(d) Relativistic effects. This is an estimated correction for the velocity dependence of the electron magnetic moment, discussed in R1 at some length; $\langle T\rangle$ is the mean kinetic energy of a single electron in a π orbital of OH, and has the approximate value $1.3\times10^{-4}mc^2$.

The two molecular matrix elements that appear in the **L**-uncoupling correction can be evaluated from experimental results: $(\Pi|L_y|\Sigma^+)$ from the measured g-factor differences and $(\Pi|BL_y|\Sigma^+)$ from the measured Λ-type doublet splittings. The value $(\Pi|L_y|\Sigma^+)=0.67\pm0.01$ was found in R1 by comparing the theoretical g-factor differences predicted by Eq. R1 (9) with the differences actually observed in the $^2\Pi_{\frac{3}{2}}$ levels. It is a particularly convincing test of the g-factor theory that this value of the matrix element, inserted in Eq. R1 (9), predicts correctly both the sign and magnitude of the two $^2\Pi_{\frac{1}{2}}$ g-factor differences; the predictions, which may be compared against Table I, are $(g_J^-g_J^+)=0.00097\pm0.00001$ for $J=\frac{3}{2}$ and $(g_J^-g_J^+)=-0.00042\pm0.00001$ for $J=\frac{5}{2}$. The second matrix element, $(\Pi|BL_y|\Sigma^+)$, can be evaluated from the Λ-type doubling parameter β_p, a derived result of the zero-field absorption experiments,[1] provided one assumes that only the single $^2\Sigma^+$ state is seriously admixed into the ground $^2\Pi$ state. With this assumption, whose validity will be examined shortly, the value of $(\Pi|BL_y|\Sigma^+)/E$ is $\frac{1}{2}(\beta_p/E)^{\frac{1}{2}}=3.84\times10^{-4}$.

The theoretical g-factor sums for $J=\frac{3}{2}$ and $J=\frac{5}{2}$ are compared with the sums of the measured g factors in Table II. For neither case is satisfactory agreement found, although the significance of the comparison for $J=\frac{5}{2}$ is obscured by the large experimental uncertainty in $\bar{g}_J(^2\Pi_{\frac{3}{2}})$. (This uncertainty comes from poor knowledge of the Λ-type doubling frequency which, not yet measured by the zero-field absorption method, had to be derived from the shift of the paramagnetic resonance spectrum produced by small changes in the observing frequency.) Obviously the theory is still inadequate but, as shown by comparing Table II with Table IV of R1, it is inadequate in a rather special way: It predicts the g-factor sums much better than it predicts the individual g factors. Since the individual g factors depend strongly on the spin coupling scheme but the sums do not, the spin-uncoupling parameter $\lambda=-7.444\pm0.017$, derived from the zero-field absorption spectrum and used to compute Table R1 IV, is clearly inconsistent with the paramagnetic resonance spectrum. For this reason λ is treated as an adjustable parameter in Sec. III.

In examining the correction terms (a)–(d) of Table II for accuracy, it is reasonable to start with the largest, doubly so because this correction, the **L**-uncoupling correction, was calculated for the simplified case of perturbation by a single excited electronic state. This is sufficient to explain the g-factor differences $(g_J^-g_J^+)$ in a very satisfying way, but it is a mistake to infer, as was done in R1, that the individual g factors (and sums of g factors) can be predicted just as precisely from the same simplified theory. The reason is that the g-factor differences do not necessarily sample all aspects of the **L**-uncoupling phenomenon, while the g factors themselves do. For it is quite likely that there should exist a nonvanishing projection of the electronic orbital angular momentum on the axis of molecular rotation, that is, a constant component of **L** in the direction of **N**. Physically, this component (hereafter called L_N) would be due to electrons bound closely to, and thus rotating in step with, the two nuclei. The rotational magnetism of such electrons would be indistinguishable from that of the rotating nuclei and, consequently, would contribute to the absolute values of the g factors without affecting the differences $(g_J^-g_J^+)$.

Any component of **L** removed from the molecular axis is a legitimate concern of the **L**-uncoupling theory; whether a constant L_N exists or not for a particular molecule it should be identifiable in the results of the general g-factor calculation carried out in R1. To see whether the calculation does in fact account for this component of **L** is not difficult: one inspects the results for electronic terms that look like nuclear rotational terms. In the g-factor sums (1) for example, there should be an electronic term with the J dependence $[J(J+1)]^{-1}[4J(J+1)-5]$, but there isn't. From the viewpoint of the perturbation theory, this missing term must be associated with perturbations by highly excited molecular states disregarded in R1; a more complete calculation, involving several excited states, would presumably generate such a term.

Certainly then it is worthwhile to see if one can match up theory and experiment by adjusting the value of g_N, specifically in the less negative direction (electron g

[4] A. A. Schupp, R. W. Pidd, and H. R. Crane, Phys. Rev. **121**, 1 (1961).

TABLE III. Theoretical g factors calculated from Eqs. (8) and (9) of reference 3 (R1), using $\lambda=-7.504$ and $g_N'=-3.7\times10^{-4}$. Sum of first five columns gives theoretical g factors in sixth column. Last column gives measured g factors. Compare with Tables IV and VII, reference 3.

$O^{16}H$ Level		g_J^0	$(\delta g_J)_s$	$(\delta g_J)_{N'}$	$\frac{1}{2}[(\delta g_J)_{L^+}+(\delta g_J)_{L^-}]$	$-g_J^0\langle T\rangle/mc^2$	$(\bar{g}_J)_{\text{th}}$	$(\bar{g}_J)_{\text{exp}}$
$^2\Pi_{\frac{3}{2}}$	$J=\frac{3}{2}$	0.93399	0.00063	−0.00018	0.00126	−0.00012	0.93557	0.93557±0.00003
	$J=\frac{5}{2}$	0.48407	0.00037	−0.00032	0.00135	−0.00006	0.48541	0.48529±0.00015
	$J=\frac{7}{2}$	0.32442	0.00027	−0.00037	0.00133	−0.00004	0.32561	0.32561±0.00004
$^2\Pi_{\frac{1}{2}}$	$J=\frac{3}{2}$	−0.13399	−0.00032	−0.00031	0.00067	0.00002	−0.13393	−0.13393±0.00002
	$J=\frac{5}{2}$	−0.14121	−0.00024	−0.00032	0.00065	0.00002	−0.14110	−0.14113±0.00003

factors are positive). Assuming the correctness of all other terms in Eq. (1), and determining an apparent nuclear rotational g factor, g_N', from the sum of the measured g factors for $J=\frac{3}{2}$, we find $g_N'=-3.7\times10^{-4}$, a change in the expected direction and by a not unreasonable amount. This makes the $J=\frac{5}{2}$ theoretical sum equal 0.34431, which still disagrees with experiment, but at least by no more than before, and still marginally within the experimental uncertainty.

2. The g Factors

For a convincing test of the value of g_N' one must turn to the several measurements of individual molecular g factors. One more adjustable parameter becomes available now, the spin uncoupling parameter λ. Table III, which is patterned after Table IV of R1, shows the overall good fit of the molecular g-factor theory to experiment when λ has the value −7.504. This was derived from the *difference* of the measured $^2\Pi_{\frac{1}{2}}$ and $^2\Pi_{\frac{3}{2}}$ g factors for $J=\frac{3}{2}$, using the above value of g_N' derived from their *sum*. The agreement of theory with experiment for the two $J=\frac{3}{2}$ levels is thus trivial, and attention should be focussed on the remaining three levels. Of these, only the $^2\Pi_{\frac{3}{2}}$, $J=\frac{5}{2}$ level shows a measured g factor notably different from the predicted value, although even here the discrepancy is within the experimental limit of error. This discrepancy, which also appears in the g-factor sum for $J=\frac{5}{2}$, should probably be considered more as evidence of an incorrect g-factor measurement than as a reason for doubting the accuracy of the predicted g factor. A zero-field measurement of the Λ-type doubling frequency would settle this question: complete consistency in Table III would require that the frequency be 6032.7 Mc/sec, as compared to the value 6033.5±1.0 Mc/sec reported in R1.

Up to this point we have considered as adjustable parameters only λ and g_N, both with good reason. In constructing Table III we have set the electron-spin g factor $g_s(\text{OH})$ equal to g_s (free) $=2(1.00116)$, the correct value for a free electron; this clearly does not disagree with the experimental results. If now one treats g_s-2 as a third adjustable parameter, it is possible to assign experimental limits of error to the equality $g_s(\text{OH})=g_s(\text{free})$. This possibility rests on the different J dependence of the g-factor corrections $(\delta g_J)_S$ and $(\delta g_J)_{N'}$ in Table III, whereby the two corrections are made experimentally distinguishable. We find that g_s-2 cannot in fact be varied by more than ±10% from the free electron value (with simultaneous adjustment of λ and g_N') without driving at least one of the five theoretical g factors out of the range allowed by experimental uncertainties. We therefore have, to fair precision, the result sought in R1, a reliable measurement of $g_s(\text{OH})$. It is $g_s(\text{OH})=g_s(\text{free})\pm0.0002=2.0023\pm0.0002$.

3. The Meaning of g_N'

The apparent nuclear rotational g factor (g_N') differs appreciably from the calculated value (g_N): According to the preceding discussion this difference can be ascribed to electrons that rotate in step with the nuclei, thereby canceling some of the true nuclear rotational magnetic moment. It should be emphasized that this effect, since it involves a component of **L** uncoupled from the molecular axis, is part of the general **L**-uncoupling phenomenon; to consider the magnetic properties of these electrons apart from the other molecular electrons is only an artifice required by imperfect knowledge of the angular wave functions. The primary significance of g_N' is thus as an empirical correction to the **L**-uncoupling calculations. The correction is plausible, but its real justification is that it works, i.e., it allows five measured g factors to be fitted by a theory involving only two adjustable parameters.

Pursuing this interpretation, one can work backwards from the confirmed existence of an N component of **L** in OH, and inquire how this would be represented by the perturbation theory. The parts of the molecular Hamiltonian responsible for **L** uncoupling admix all of the excited $^2\Sigma$ and $^2\Delta$ states into the ground $^2\Pi$ state, and the formal contribution of each to the ground state g factors resemble superficially the expressions for $(\delta g_J)_{L^\pm}$ given in R1. There are important differences, however, which show up most clearly in the g-factor sums: each $^2\Sigma$ state, whether of the $^2\Sigma^+$ or $^2\Sigma^-$ type, perturbs the g-factor sums by adding a term to Eq. (1) of the form

$$\frac{2[4J(J+1)-1]}{J(J+1)}\frac{(\Pi|L_y|\Sigma)(\Sigma|BL_y|\Pi)}{E_\Sigma-E_\Pi}, \tag{2}$$

while each $^2\Delta$ state contributes a term of the form

$$\frac{2[4J(J+1)-9]}{J(J+1)}\frac{(\Pi|L_y|\Delta)(\Delta|BL_y|\Pi)}{E_\Delta-E_\Pi}; \tag{3}$$

the pertinent difference is that Eq. (3) has a 9 where Eq. (2) has a 1. The g-factor differences are also affected unequally: $^2\Sigma^+$ states make positive contributions to $(g_J^- - g_J^+)$, while $^2\Sigma^-$ states make negative contributions identical in form but for the sign reversal. The $^2\Delta$ states, on the other hand, perturb both g_J^+ and g_J^- equally, and thus do not affect the differences. These results are all based on second-order perturbation calculations, and are correct only to the extent that higher order perturbations are, as is here the case, negligible.

From this information, and unhampered by experimental knowledge of the types and locations of the highly excited states, one can easily construct a g-factor perturbation with the two required properties—one which (1) contributes nothing to the g-factor differences and (2) adds to the g factors themselves a term resembling the nuclear rotation correction. For these conditions to be satisfied it is necessary and sufficient that the strengths of perturbations by $^2\Sigma^+$, $^2\Sigma^-$, and $^2\Delta$ states be in the proportion 1:1:2. If, furthermore, the composite correction to the g-factor sums is written as $\frac{1}{2}g_N{}^e[J(J+1)]^{-1}[4J(J+1)-5]$ to match exactly the nuclear rotation correction, then one has the following two relations for $g_N{}^e$, the electronic contribution to the apparent nuclear rotational g factor:

$$g_N{}^e = 8 \sum_{\Delta \text{ states}} (\Pi|L_y|\Delta)(\Delta|BL_y|\Pi)/(E_\Delta - E_\Pi),$$

$$8 \sum_{\Sigma \text{ states}}{}' (\Pi|L_y|\Sigma)(\Sigma|BL_y|\Pi)/(E_\Sigma - E_\Pi) \leq g_N{}^e \qquad (4)$$

$$\lesssim 16 \sum_{\Sigma \text{ states}}{}' (\Pi|L_y|\Sigma)(\Sigma|BL_y|\Pi)/(E_\Sigma - E_\Pi).$$

The primed sum over Σ states means that the state (in OH, the lowest $^2\Sigma^+$) that contributes the dominant term in the sum must be excluded. Only a small fraction of its total perturbation of the ground state enters the description of L_N, specifically, that fraction required to cancel out the residual Σ^+ or Σ^- character of the net perturbation by higher states which, if uncanceled, would contribute to the g-factor differences. By omitting this term, however, one also underestimates the size of $g_N{}^e$ by an unknown amount which does not exceed approximately 50% (as would be the case if the primed sum contained only one important term); this uncertainty has been accounted for in Eq. (4).

It still remains to fit together the two perturbation calculations—the *a priori* calculation which involves only the first-excited state and the present *ad hoc* calculation which brings in all of the other excited states. The problem is that, as mentioned above, a small part of the perturbation by the first excited state may be common to both the *a priori* and the *ad hoc* calculations. That is, by considering in R1 only the first-excited state, we have already accounted partially for L_N; thus it might appear doubtful that the value of g_N' derived by comparing the *a priori* calculation with the observed spectrum actually measures the quantity $g_N + g_N{}^e$, where $g_N{}^e$ is given by Eq. (4).

The situation is saved by the fact that the Λ-type doubling separations, like the g-factor differences, measure only that part of the total perturbation by excited Σ states that has an uncompensated Σ^+ or Σ^- character. The Λ-type doubling parameter β_p, for instance, is defined by[1]

$$\beta_p \equiv 4 \sum_{\Sigma \text{ states}} (-1)^s |(\Pi|BL_y|\Sigma)|^2/(E_\Sigma - E_\Pi), \qquad (5)$$

where the exponent on (-1) is an even integer for Σ^+ states and an odd integer for Σ^- states. The same sort of partial cancellation occurs in the definition of α_p, the other parameter involved in the Λ-type doubling. Thus the values of α_p and β_p derived from the Λ-type doubling measurements, when combined with the g-factor theory of R1, do not specify completely the magnetic perturbation by the first-excited state; they leave out precisely that part that enters the perturbation description of L_N, the part that is *included* by the *ad hoc* calculation. We conclude that the apparent nuclear rotational g factor, g_N', does indeed contain the total magnetic contribution of L_N, and thus may be compared directly with $g_N + g_N{}^e$. This gives the experimental value $g_N{}^e = 1.7 \times 10^{-4}$.

The information on molecular wave functions or energy levels to be gained by substituting this value of $g_N{}^e$ into Eq. (4) is clearly negligible without knowledge of the excitation energies involved. More interesting is the extra information that is now available on the dominant perturbation by the lowest $^2\Sigma^+$ state. On extracting the dominant term, Eq. (5) becomes

$$4|(\Pi|BL_y|\Sigma^+)|^2/E$$
$$= \beta_p - 4 \sum_{\Sigma \text{ states}}{}' (-1)^s |(\Pi|BL_y|\Sigma)|^2/(E_\Sigma - E_\Pi)$$
$$\simeq \beta_p - 4B_p \sum_{\Sigma \text{ states}}{}' (-1)^s (\Pi|L_y|\Sigma)(\Sigma|BL_y|\Pi)/(E_\Sigma - E_\Pi), \qquad (6)$$

where E is the known excitation energy of the first-excited $^2\Sigma^+$ state and the pure precession hypothesis[5] (discussed below) has been invoked to take out one of the Bs. Now the remaining primed sum will have a value that falls somewhere in the range between zero and $-g_N{}^e/16$. Choosing the middle value as the most likely, but including an uncertainty large enough to account for any eventuality, one then has $4|(\Pi|BL_y|\Sigma^+)|^2/E = \beta_p + (1 \pm 1)B_p g_N{}^e/8$. The magnitude of the matrix element $(\Pi|BL_y|\Sigma^+)$, found by substituting measured values of E, β_p, B_p, and $g_N{}^e$ into this expression, is 12.65 ± 0.13 cm^{-1}.

The use of the pure precession hypothesis in Eq. (6) may now be justified in retrospect. As ordinarily used,

[5] J. H. Van Vleck, Phys. Rev. **33**, 467 (1929).

this hypothesis has two parts: One assumes, in calculating off-diagonal matrix elements like $(\Pi|BL_y|\Sigma)$, that (1) the rotational operator B may be taken outside and given its measured diagonal value (B_p, if one is concerned with the Π state) and (2) that $\mathbf{L}^2$ has the constant value $L(L+1)$, where L is taken to be unity for the $\Pi-\Sigma$ perturbation; the latter assumption yields the value $\sqrt{2}/2$ for the orbital matrix element $(\Pi|L_y|\Sigma)$. The predicted value of the matrix element $(\Pi|BL_y|\Sigma^+)$, based on these two assumptions, is 13.1 cm^{-1}, which disagrees by less than 4% with the measured value. The discrepancy can be reduced still further if one uses, in place of assumption (2), the experimental result $(\Pi|L_y|\Sigma^+)=0.67\pm0.01$ derived from the g-factor differences; the predicted value of $(\Pi|BL_y|\Sigma^+)$ is then 12.4 ±0.2 cm^{-1}, in satisfactory agreement with experiment.

A further comparison of g_N' with theory may be had if one returns to the original picture of electrons localized on the two nuclei, and rotating in step with them; this point of view, with its greater physical immediacy, draws its significance from the perturbation theory result that g_N' includes the entire electronic contribution to the "nuclear" rotational g factor. Since in OH the proton executes practically all of the nuclear rotational motion, the electrons that contribute to g_N' must be localized on the proton, i.e., they can be thought of as occupying s orbitals of the hydrogen atom. These electrons reduce the effective charge-to-mass ratio of the rotating proton, thereby reducing the nuclear rotational magnetic moment. The observed fractional reduction in the magnetic moment thus measures the electron population of atomic hydrogen s orbitals in OH; from the value of $(g_N-g_N')/g_N$ this population is 0.32. This figure may be compared directly with a theoretical value of approximately 0.64, taken from a LCAO (linear combination of atomic orbitals) calculation of OH wave functions.[6] Some of the discrepancy may be accountable by effects of configuration interaction which, as will be seen from the next section, are rather pronounced in OH.

4. Hyperfine Structure

In R1 it was found that the hfs splittings in the $^2\Pi_{\frac{3}{2}}$ paramagnetic resonance spectra of both OH and OD were consistent with the following values of four hfs coupling constants: $a(\mathrm{OH})=48.7\pm0.5$ Mc/sec, $b(\mathrm{OH})=113.6\pm0.6$ Mc/sec, $c(\mathrm{OH})=-25\pm5$ Mc/sec, and $d(\mathrm{OH})=57.0\pm1.5$ Mc/sec. The constant a measures the interaction of the proton magnetic dipole moment with the magnetic field generated by electronic orbital motion, the remaining constants measure the anisotropic (dipole-dipole) and isotropic (relativistic) interactions between the proton moment and the spin magnetic moments of unpaired electrons; the coupling constants are defined by Eq. (11) of R1, and Eq. (12) shows how they combine to yield the specific hfs constants A_1 and A_2 of a given rotational level.[7] The values of A_1 and A_2 measured from the $^2\Pi_{\frac{3}{2}}$ spectra are, however, noncommital with regard to the precise numerical values of a and c; to get the above values one must make the further assumption that a involves the same electrons as do c and d, which leads to the additional relation $c=3(a-d)$. This assumption is prompted by the simplest picture of the electronic structure of OH, in which one π electron carries the orbital angular momentum, a second equivalent π electron carries the unpaired spin.

TABLE IV. Magnetic hyperfine structure coupling constants calculated from Eq. (12b) of reference 3 (R1), using the values $a(\mathrm{OH})=86.0$ Mc/sec, $b(\mathrm{OH})=-119.0$ Mc/sec, $c(\mathrm{OH})=133.2$ Mc/sec. All entries in Mc/sec.

Level		$(A_1)_{\mathrm{calc}}$	$\lvert A_1\rvert_{\mathrm{calc}}-\lvert A_1\rvert_{\mathrm{exp}}$
$O^{16}H\ ^2\Pi_{\frac{3}{2}}$	$J=\frac{3}{2}$	27.01	0.00
	$J=\frac{5}{2}$	5.32	−0.08
	$J=\frac{7}{2}$	−1.09	−0.09
	$J=\frac{9}{2}$	−3.43	+0.30[a]
$^2\Pi_{\frac{1}{2}}$	$J=\frac{3}{2}$	20.72	+0.17
	$J=\frac{5}{2}$	15.14	0.00
$O^{16}D\ ^2\Pi_{\frac{3}{2}}$	$J=\frac{3}{2}$	4.78[b]	−0.06

[a] In reference 1 the hfs interval $\Delta\nu_s=31.3\pm0.8$ Mc/sec measured in the $J=9/2$ level is equal to $(2J+1)|A_1|$ in the present notation, i.e., from reference 1, $|A_1|=3.13\pm0.08$ Mc/sec for $J=9/2$.
[b] Calculated from the relation $a(\mathrm{OD})=[g_I(\mathrm{D})/g_I(\mathrm{H})]a(\mathrm{OH})$ and corresponding relations for b(OD) and c(OD).

The new hfs data allow one to set a free of c and derive a new set of coupling constants, subject to no assumptions about electronic structure, from Eq. R1 (12) [corrected as noted in footnote 7] and the combined $^2\Pi_{\frac{1}{2}}$ and $^2\Pi_{\frac{3}{2}}$ measurements. Radically different from the earlier values, they are:

$$a(\mathrm{OH})=\ 86.0\pm0.6\ \mathrm{Mc/sec},$$
$$b(\mathrm{OH})=-119.0\pm0.4\ \mathrm{Mc/sec},$$
$$c(\mathrm{OH})=\ 133.2\pm1.0\ \mathrm{Mc/sec},$$
$$d(\mathrm{OH})=\ 56.5\pm0.4\ \mathrm{Mc/sec}.$$

Limits of error have been chosen conservatively to account for the neglect of certain off-diagonal matrix elements in the calculation of Eq. R1 (12). A more accurate calculation of the hfs, including these off-diagonal matrix elements, is not justified by the precision of the present measurements. Table IV, patterned after Table VI of R1, shows the consistency of the new values of a, b, and c with all available measurements of A_1, including a single zero-field measurement on the $^2\Pi_{\frac{3}{2}}$, $J=\frac{9}{2}$ level. Table V does the same for A_2, the theoretical values of which depend only on d. Comparable values of $A_2[=\Delta\nu_1/(2J+1)]$ taken from zero-field measurements are also included in Table V; these agree within ex-

[6] A. J. Freeman, J. Chem. Phys. 28, 230 (1958); Ordnance Materials Research Laboratory Report No. 28, 1957 (unpublished).

[7] The sign correction mentioned after Eq. (12b) is uncalled for, and the term $4(J+\frac{3}{2})(J-\frac{1}{2})$ should be preceded by a + sign, as given originally in reference 1. This sign change inverts the signs of the derived hyperfine structure constants b and c but, as it happens, alters their magnitudes only slightly. The derived values of a and d are not affected.

TABLE V. Comparison of observed hyperfine doubling with theory and with zero-field measurements by other investigators. The values of $(A_2)_{calc}$ are calculated from Eq. (12b) of reference 3 (R1) using the value $d(OH)=56.5$ Mc/sec. All entries in Mc/sec.

Level		$(A_2)_{calc}$	$(A_2)_{exp}$	$\Delta\nu_1/(2J+1)$[a]
$O^{16}H\ ^2\Pi_{\frac{3}{2}}$	$J=\frac{3}{2}$	0.45	0.51±0.05	0.47±0.03[c]
	$J=\frac{5}{2}$	0.68	0.68±0.05	
	$J=\frac{7}{2}$	0.81	0.87±0.05	0.84±0.01[d]
$^2\Pi_{\frac{1}{2}}$	$J=\frac{3}{2}$	14.58	14.56±0.05	14.89±0.06[d]
	$J=\frac{5}{2}$	9.00	9.03±0.03	8.91±0.04[d]
$O^{16}D\ ^2\Pi_{\frac{3}{2}}$	$J=\frac{3}{2}$	0.03[b]	0.03±0.03	

[a] The frequency splittings $\Delta\nu_1$ measured in the zero-field experiments are equal to $(2J+1)A_2$ in the present notation.
[b] Calculated with the relation $d(OD)=[g_I(D)/g_I(H)]d(OH)$.
[c] Taken from reference 2.
[d] Taken from reference 1.

perimental error for the $^2\Pi_{\frac{3}{2}}$ levels, but not for the $^2\Pi_{\frac{1}{2}}$ levels. The origin of the latter discrepancy is not clear, but it should be noted that the paramagnetic resonance values of A_2 for the $^2\Pi_{\frac{1}{2}}$ levels are at least consistent with a single value of d, while the zero-field values are not.

The extreme insensitivity of the $^2\Pi_{\frac{3}{2}}$ hfs splittings to changes in the values of a and c may be seen by comparing Table IV with Table VI of R1: both the new and old sets of coupling constants account for the $^2\Pi_{\frac{3}{2}}$ splittings equally well. Indeed, only the presumed relation $c=3(a-d)$ has been violated in fitting the hfs theory to the present $^2\Pi_{\frac{1}{2}}$ measurements. Clearly, from the size of this violation, it is only a crude approximation to say that in OH the same electrons carry both the orbital and spin angular momentum. Put more precisely, the ground electron configuration of OH,

$$(1\sigma)^2(2\sigma)^2(3\sigma)^2(\pi^+)^2\pi^-,$$

can account only partially for the observed hyperfine structure; one must also consider excited configurations which may contain unpaired electrons in several different orbitals and which, having $^2\Pi$ symmetry, can contribute to the formation of the ground state. Theoretical investigations[8] of this "configuration interaction" for OH show that the excited configurations formed by promoting σ electrons to higher, normally vacant σ orbitals are in fact admixed to a considerable extent, the total energy of the ground state being thereby lowered. The unpaired σ electrons of such configurations will contribute to the spin part of the hfs interaction (coupling constants b, c, d) but not to the orbital part (coupling constant a), thereby invalidating the relation $c=3(a-d)$.

The present hfs data, apart from showing with certainty its presence, say little about the details of this configuration interaction. The measured values of a, b, c, and d should be regarded rather as tests for OH wavefunctions calculated from first principles. Nevertheless, a crude phenomenological analysis is helpful in estimating the contribution of σ electrons to the measured coupling constants. Instead of the single-electron definitions of the coupling constants given by Eq. (11b) of R1, it is clearly preferable to write them as

$$\begin{aligned} a&=a_\pi=2g_I\mu_0^2\langle 1/r^3\rangle_\pi,\\ b&=b_\pi+b_\sigma+F=-g_I\mu_0^2\langle(3\cos^2\chi-1)/r^3\rangle_\pi+b_\sigma\\ &\qquad+(16\pi/3)g_I\mu_0^2\Psi^2(0), \quad (7)\\ c&=c_\pi+c_\sigma=3g_I\mu_0^2\langle(3\cos^2\chi-1)/r^3\rangle_\pi+c_\sigma,\\ d&=d_\pi+d_\sigma=3g_I\mu_0^2\langle\sin^2\chi/r^3\rangle_\pi+d_\sigma, \end{aligned}$$

where b_σ represents a sum over σ electrons of terms like $g_I\mu_0^2\langle(3\cos^2\chi-1)/r^3\rangle_\sigma$ with appropriate coefficients, and c_σ and d_σ are to be interpreted in a similar fashion. (The distance r is measured from the magnetic nucleus to the interacting electron, and χ is the angle included by r and the molecular axis.) Both π and σ electrons may contribute to the isotropic interaction constant F (for Fermi), but it is unnecessary to make this distinction in Eq. (7), since the parameter $\Psi^2(0)$, the electron density at the magnetic nucleus, includes both with equal facility. Identifying c_σ with $-3b_\sigma$, one can write immediately $F=b+c/3$; with the correct experimental values of b and c this gives $F=-74.6\pm0.6$ Mc/sec. The significance of the minus sign is discussed below.

Experiment alone offers no way of distinguishing between the π and σ contributions to b, c, and d; rather, to achieve the desired separation one must rely on theoretical calculations of the π contributions. Fortunately, the measured value of $a(=a_\pi)$ gives an independent check of such calculations, for wave functions that account for a_π should also yield correct values for b_π, c_π, and d_π. The simple LCAO wave function discussed in R1 would seem to be quite adequate for this purpose: from values of $\langle 1/r^3\rangle$ and $\langle\sin^2\chi/r^3\rangle$ calculated there the theoretical coupling constants a_π and d_π are respectively 87 Mc/sec (as compared to the measured 86.0±0.6 Mc/sec) and 47 Mc/sec. The theoretical values of b_π and c_π, determined by the relations $b_\pi=-c_\pi/3$ and $c_\pi=3(a_\pi-d_\pi)$ [which is correct, although $c=3(a-d)$ is not] are −40 Mc/sec and 120 Mc/sec. Inserted in Eq. (7), these values give $b_\sigma\simeq-4.4$ Mc/sec, $c_\sigma\simeq13$ Mc/sec, and $d_\sigma\simeq10$ Mc/sec. Thus configuration interaction in OH appears to be responsible for about 10% of the observed anisotropic hyperfine structure interaction.

The single-configuration LCAO wave function that predicts so well the value of a_π fails completely when it comes to the isotropic coupling constant F. This is because the single unpaired electron of the ground configuration, a π electron, is represented in the LCAO scheme by a $2p$ orbital of the oxygen atom, which vanishes along the molecular axis. Although the $2p$ orbit will actually be distorted somewhat by the presence of the hydrogen nucleus, it is unlikely that any resulting value of $\Psi^2(0)$ could account for more than a small part of the measured isotropic coupling constant. Rather, the experimental value of F should be regarded as a reasonably accurate measure of the extent of configuration

[8] M. Krauss and J. F. Wehner, J. Chem. Phys. **29**, 1287 (1958).

TABLE VI. Molecular parameters of $O^{16}H$. Major results derived from the paramagnetic resonance spectra together with comparable results of other experiments and theoretical predictions.

	Parameter	Paramagnetic resonance	Zero-field[a] microwave absorption	Optical[b] emission	Theory
	g_s(OH)	g_s(free)$\pm$0.0002			g_s(free)
	λ	-7.504 ± 0.003	-7.444 ± 0.017	-7.547	
	$(\Pi\|L_y\|\Sigma^+)$	0.67 $\pm$0.01			0.707[c]
	$(\Pi\|BL_y\|\Sigma^+)$	12.65 $\pm$0.13 cm^{-1} [d]			13.1 cm^{-1} [c]
Σ Δ states	$\dfrac{(\Pi\|L_y\|\Delta)(\Delta\|BL_y\|\Pi)}{E_\Delta - E_\Pi}$	1.7 $\times10^{-4}$			
	$\langle 1/r^3\rangle_\pi$	$(1.089\pm0.008)\times10^{24}$ cm^{-3}	$(0.75\ \pm0.25)\times10^{24}$ cm^{-3}		1.1×10^{24} cm^{-3} [e]
	$\Psi^2(0)$	$(0.113\pm0.001)\times10^{24}$ cm^{-3}			0[e]
	$\langle(3\cos^2\chi-1)/r^3\rangle$	$(1.125\pm0.008)\times10^{24}$ cm^{-3}			1.0×10^{24} cm^{-3} [e]
	$\langle\sin^2\chi/r^2\rangle$	$(0.477\pm0.003)\times10^{24}$ cm^{-3}	$(0.490\pm0.013)\times10^{24}$ cm^{-3}		0.4×10^{24} cm^{-3} [e]

[a] Reference 1.
[b] G. H. Dieke and R. M. Crosswhite, Bumblebee Report No. 87, Johns Hopkins University, Nov. 1948 (unpublished).
[c] Pure precession value.
[d] Calculated from the value of β_p given in reference 1 after subtracting the contribution of other excited states.
[e] LCAO calculation, neglecting configuration interaction.

interaction, the presence of which has already been detected in the anisotropic coupling constants. That F turns out to be negative for OH, seemingly implying a negative value for $\Psi^2(0)$, would be alarming were it not for recent calculations by Goodings[9] on "core polarization" in atoms. Goodings finds that core polarization (configuration interaction) in light P state atoms may produce isotropic hyperfine structure with negative coupling constants, although of course the value of $\Psi^2(0)$ remains positive definite. It appears likely that a careful calculation of configuration interaction in OH, a light Π state molecule, would yield the same result.

In terms of molecular constants, the final results of the analysis of the OH (and OD) hyperfine structure are:

$$\langle 1/r^3\rangle_\pi = (1.089\pm0.008)\times10^{24}\ \text{cm}^{-3},$$
$$\langle(3\cos^2\chi-1)/r^3\rangle = (1.125\pm0.008)\times10^{24}\ \text{cm}^{-3},$$
$$\langle\sin^2\chi/r^3\rangle = (0.477\pm0.003)\times10^{24}\ \text{cm}^{-3},$$
$$\Psi^2(0) = (0.113\pm0.001)\times10^{24}\ \text{cm}^{-3},$$

where $\langle 1/r^3\rangle_\pi$ refers to a single π electron but the remaining constants represent summations over all unpaired electrons.

IV. RESULTS AND DISCUSSION

The major objective of these experiments, to measure the electron spin magnetic moment in the intense axially symmetric electric field of a diatomic molecule, has been achieved reasonably well. To a precision of 1 part in 10^4, sufficient to detect a 10% alteration of the spin moment anomaly (g_s-2), the fundamental magnetic properties of an electron bound in the OH molecule are found to be the same as those of a free electron. In view of the similar conclusion reached after extensive study of the diatomic oxygen molecule,[10] this result is certainly not unexpected; yet it should be re-emphasized that in OH the electron spin magnetic moment is coupled more tightly to the internuclear electric field than it is in O_2, and therefore should feel its effects, if any, more strongly. The coupling is of course indirect in both molecules, but it occurs in OH via the spin-orbit interaction (coupling constant $\sim$140 cm^{-1}), in O_2 via the much weaker spin-spin interaction (coupling constant $\sim$2 cm^{-1}). For this reason the OH molecule offers, at least potentially, a much more sensitive test of a possible environmental effect on the electron-spin magnetic moment. The major difficulty in exploiting this test has been, and continues to be, the complex vector coupling scheme of OH. The present measurement of g_s(OH) suffers from the fact that most of the experimental data had to be used up in a simultaneous measurement of the coupling scheme.

The wave function information provided by this experiment is of two sorts: The observed Zeeman effect yields parameters that specify in great detail the angular dependence, relative to the internuclear axis, of the molecular wavefunctions (the vector coupling scheme); the observed hyperfine structure yields parameters that describe both the angular and the radial dependence of the wavefunctions with respect to a coordinate system centered in the hydrogen nucleus. These molecular parameters are collected in Table VI, together with comparable results of other experiments and theoretical predictions, where available.

The principal molecular parameter measured by the Zeeman effect is λ, the ratio of the spin-orbit coupling constant of the ground state to its rotational constant. There is a real and disturbingly large difference between the two microwave values of λ in Table VI; the paramagnetic resonance value differs from the zero-field

[9] D. A. Goodings, Phys. Rev. **123**, 1706 (1961).

[10] K. D. Bowers, R. A. Kamper, and C. D. Lustig, Proc. Roy. Soc. (London) **A251**, 565 (1959).

value by 0.8%, almost four times the experimental uncertainty in the latter. This discrepancy was noted previously in R1 but, because of uncertainty about the proper interpretation of the experiment, there remained some doubt of its reality at that time.

There seems to be no compelling reason to prefer one value over the other: The two experiments are quite similar in technique and experimental precision, and agreement is found at several points where direct measurements can be compared; the two values of λ result from well-grounded theoretical analyses of the spectra which, in both cases, show a high degree of internal consistency over several molecular levels. We can only conclude that there remains a flaw, undetectable by internal consistency checks, in the theoretical treatment of either the Zeeman effect or the Λ-type doubling. Table VI also shows that the two microwave values of λ, discordant themselves, also fail to agree with the optically measured value. The uncertainty in the optical number, however, is estimated[1] to be as much as 1%; this covers adequately the paramagnetic resonance result, marginally the zero-field microwave result.

Apart from the numerical value of λ and the question of the correct value for the Λ-type doubling frequency of the $^2\Pi_{\frac{3}{2}}$, $J=\frac{5}{2}$ level, there are no remaining difficulties in the interpretation of the OH paramagnetic resonance spectra, at least to the precision attained in the present experiments. This precision could perhaps be improved by a factor of ten with moderate effort, but there is little point in doing so without a detailed calculation of relativistic corrections to the molecular Zeeman effect. This is a difficult problem, made more difficult for OH by the apparent seriousness of configuration interaction effects. Although the sort of configuration interaction discussed above does not affect the angular properties of the molecular wavefunctions, and hence cannot perturb the nonrelativistic Zeeman effect, it can enter the relativistic corrections through quantities such as electron kinetic energies which, like the hfs coupling constants, depend on details of the electron distribution.

PHYSICAL REVIEW VOLUME 126, NUMBER 3 MAY 1, 1962

Elastic Scattering at Resonance from Bound Nuclei

G. T. TRAMMELL
Oak Ridge National Laboratory, Oak Ridge, Tennessee
(Received June 5, 1961)

The usual Debye-Waller factor, $\langle\exp[-i(\mathbf{k}_f-\mathbf{k}_0)\cdot\mathbf{r}]\rangle$, which when multiplying the fixed-scatterer amplitude gives the nonresonant elastic-scattering amplitude from a bound scatterer, is generally applicable only for fast collisions, i.e., if the "collision time," $\hbar(d/dE)$(scattering phase shift), is much less than a characteristic vibration time, ω_m^{-1}, of the bound scatterer about its mean position. In the opposite extreme case, where the "collision time" is very long compared to ω_m^{-1} (slow collisions), there is negligible correlation between the positions of absorption and subsequence re-emission (for an atom bound in a crystal), and the "Debye-Waller" factor becomes $\langle\exp(-i\mathbf{k}_f\cdot\mathbf{r})\rangle\langle\exp(i\mathbf{k}_0\cdot\mathbf{r})\rangle$. If the scatterers' surroundings exhibit cubic symmetry, the extremes as well as all intermediate cases give the same factor for 90° scattering angle. In the case of medium collisions, collision time ≈ vibration time, the elastic scattering amplitude becomes sensitive to the detailed vibrational spectrum of the bound scatterer. For nonresonant scattering the collision times are of the order of transit times (x ray across the atom for Thomson scattering, neutron across the nucleus for neutron potential scattering) and are thus fast collisions.

The inverse characteristic vibration times of atoms in crystals are of the order of their Debye Θ and are a few hundredths of an ev. Slow neutron nuclear resonance widths vary from a few hundredths to a few tenths ev; therefore slow neutron collisions are medium to fast. Gamma-ray resonances for $E_\gamma<100$ kev (Mössbauer), on the other hand, have widths less than 10^{-5} ev, and therefore correspond to slow collisions.

A slight generalization of a formula due to Lamb gives the resonant scattering, and our discussion of the formula is largely a straightforward extension of those of Lamb and Singwi and Sjölander in their discussion of resonance absorption. The total absorption cross section and, in most cases of interest, the inelastic scattering cross section may be obtained from the elastic scattering amplitude.

I. INTRODUCTION

THE waves which are elastically scattered from the various atoms of crystal interfere to give the Laue or Bragg diffraction pattern, and it is from this that their chief interest and usefulness derives.[1] The studies of chemical and magnetic structures of crystals by means of x ray and neutron diffraction techniques are too numerous and well known to require discussion here. It is sufficient to mention that the x-ray scattering is usually mainly given by the Thomson scattering from the atomic electrons, while the neutron scattering is given by the nuclear (potential) scattering and, in the case of magnetic materials, the magnetic electron scattering.

Recently Moon and collaborators[2] have demonstrated

[1] The elastic scattering also generally has an incoherent part, due to spin effects or crystal imperfections, which contributes a diffuse background between the Bragg peaks. The inelastic scattering, wherein phonons are created or absorbed in the crystal, generally has a coherent component which, however, because of the near continuum of the phonon momentum spectrum, appears as a diffuse background around the Bragg peaks.

[2] P. J. Black and P. B. Moon, Nature **188**, 481 (1960).